Diagnostic and Interventional Imaging (2019) **100**, 95—107

ORIGINAL ARTICLE / *Thoracic imaging*

Influence of radiologic expertise in detecting lung tumors on chest radiographs

H. Takahashi[a,b,*], **M. Kiyoshima**[c], **T. Kaburagi**[d], **S. Hoshiai**[a,b], **K. Mori**[a], **K. Koyama**[b], **T. Iijima**[e], **T. Ishiguro**[a], **T. Hosokawa**[f], **M. Minami**[a]

[a] *University of Tsukuba, Faculty of Medicine, Department of Diagnostic and Interventional Radiology, Ibaraki, Japan*
[b] *Ibaraki Prefectural Central Hospital, Department of Diagnostic and Interventional Radiology, Ibaraki, Japan*
[c] *Ibaraki Prefectural Central Hospital, Department of Thoracic Surgery, Ibaraki, Japan*
[d] *Ibaraki Prefectural Central Hospital, Department of Respiratory Medicine, Ibaraki, Japan*
[e] *Ibaraki Prefectural Central Hospital, Department of Pathology, Ibaraki, Japan*
[f] *Saitama Children's Medical Center, Department of Radiology, Saitama, Japan*

KEYWORDS
Chest radiography;
Training regimen;
Education;
Pulmonary nodule detectability

Abstract
Purpose: To analyze the influence of radiologic expertise in detecting lung tumors on chest radiographs.
Materials and methods: We retrieved posteroanterior chest radiographs and CT examination obtained from 283 patients with solitary primary malignant lung tumors who underwent surgical resection. There were 176 men and 107 women with a mean age of 67.0 ± 9.1 (SD) years (range: 33—88 years). Thirteen first-year post-graduate (PGY-1) trainees and nine pulmonary specialists (three radiologists, three thoracic surgeons, and three pulmonologists) interpreted the chest radiographs. Detection rates among trainees and specialists were compared using Student *t* test.
Results: The total numbers of detected tumors ranged from 103 (36.4%) to 136 (48.1%) with a mean of 127.9 ± 9.1 (45.2 ± 3.2%) in the trainee group, and 137 (48.4%) to 182 (64.3%) with a mean of 161.6 ± 13.1 (57.1 ± 4.6%) in the specialist group; the intergroup difference was statistically significant ($P < 0.001$). Significant intergroup detectability differences of >10% were noted for tumors in the peripheral zone with (i) ground glass opacity (GGO) ratio ≥10% and <70% and any size, or (ii) GGO ratio <10% and size ≤2 cm; and for tumors hidden by the mediastinum, heart, or diaphragm with (i) GGO ratio ≥10% and <30% and size >3 cm, or (ii) GGO ratio <10% and size >2 cm.

* Corresponding author. University of Tsukuba, Faculty of Medicine, Department of Diagnostic and Interventional Radiology, 1-1-1, Tennoudai, 3058575 Tsukuba, Ibaraki, Japan.
E-mail address: h.1982.takahashi@gmail.com (H. Takahashi).

https://doi.org/10.1016/j.diii.2018.08.015

Conclusion: Our study demonstrates significant differences in lung tumor detectability on chest radiographs between PGY-1 trainees and pulmonary specialists according to tumor size, extent of GGO, and tumor location.

Chest radiography remains the initial imaging modality for the investigation of lung abnormalities, although the utility of chest radiography for the screening of lung abnormalities is limited due to its low diagnostic capability [1—4]. Notably, chest radiography is commonly used in daily routine and is the second-most frequently used medical test, after electrocardiogram [5]. Therefore, the ability to read chest radiography is required, not only for specialists in radiology or pulmonology, but for physicians with other specialty. In addition, it has been demonstrated that technical inaccuracies of image interpretation are a major reason for misdiagnoses on chest radiographs [6—9]; increasing chest radiograph interpretation skills requires abundant experience and training that results in more effective use of visual search [10,11]. Therefore, chest radiography remains a ''must-learn'' topic in post-graduate training.

Currently, however, the time involved in training of chest radiography has been reduced, because of training for other types of image interpretation [5,12]. Fabre et al. demonstrated a lack of skills among residents for reading chest radiographs related to theoretical background, and suggested the importance of training courses for chest radiographs in residency programs [12]. Therefore, effective measures must be implemented to ensure that physicians in training, who must have a large knowledge but can spend a limited period of time for studying radiological image interpretation, receive appropriate training for the skills required to interpret chest radiographs. Notably, understanding the imaging characteristics of lung lesions that cause differences in detectability between experts and non-experts would contribute to rational case selection for training regimens involving chest radiographs.

Previous reports have demonstrated that the tumor size, extent of ground glass opacity (GGO), and tumor location can affect the detectability of lung tumors on chest radiographs [6—8,13—16]. However, it is unclear how these factors affect the detectability according to reader expertise.

The goal of this study was to analyze the influence of radiologic expertise in detection of lung tumors on chest radiographs by comparing detection rates between first-year post-graduate (PGY-1) trainees and pulmonary specialists, including radiologists, thoracic surgeons, and pulmonologists.

Materials and methods

This study was approved by the appropriate Institutional Review Board, which waived the requirement for written informed consent due to the retrospective nature of the study.

Patients

Among patients presenting with surgically resected, solitary primary malignant lung tumors between January 2011 and December 2014, the data of 283 patients who underwent preoperative posteroanterior (PA) chest radiography and computed tomography (CT) examination were retrieved. We excluded patients with multiple lung tumors, past thoracic surgery, calcified tumors, tumor-related atelectasis, and obstructive pneumonia, which were found on CT examinations. Histologic types of all surgically resected specimens were determined on the basis of the 2015 WHO Classification of Tumors of the Lung, Pleura, Thymus and Heart [17]. The patients consisted of 176 men and 107 women with a mean age of 67.0 ± 9.1 (SD) years (range: 33—88 years). The interval between preoperative chest radiography and preoperative CT examination ranged from 0 to 76 days (mean, 15 days). All chest radiographs were anonymized and saved in DICOM format.

Image acquisition

PA chest radiographs were obtained in the upright position at 120 kVp with automatic exposure control (Hitachi DHF-158 HII, Hitachi) and a 10:1 grid (Konica FDP, Konica-Minolta). CT examinations were performed with 128 or 32 detector rows (Somatom Definition Flash® or Biograph mCT®; Siemens Healthineers). The collimation width of each detector row was 0.6 mm. In all patients, CT scans were performed in the supine position under breath-holding in full inspiration without intravenous injection of iodinated contrast agents. The beam pitch was 0.6 to 1.2. Contiguous 1 mm thick axial CT images in the lung and mediastinal window settings were reconstructed without using the iterative reconstruction technique.

Image analysis

Areas on chest radiographs were classified into three main zones and 11 regions (Fig. 1). The three main zones, the peripheral, central and apical, and hidden zones, were divided according to the amount of anatomical noise. The peripheral zone showed the least anatomic noise. The central and apical zone were partly hindered by clavicles or hilar vessels. The hidden zone was entirely hindered by the heart, mediastinum, or diaphragm. The boundaries of the medial

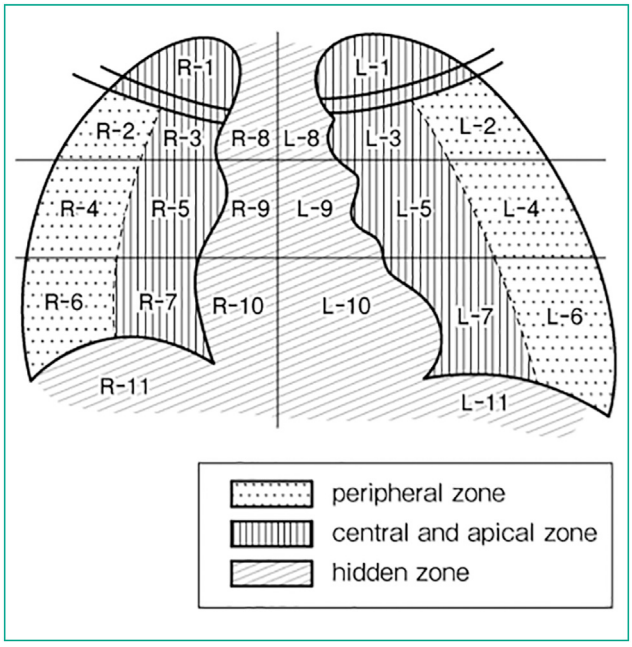

Figure 1. The location scheme of the chest radiograph. Three main zones and 11 regions on both sides are shown. The 11 regions of the right (R-) and left (L-) lung were as follows: the apical lung region (R-1 and L-1), the upper lateral lung region (R-2 and L-2), the upper medial lung region (R-3 and L-3), the middle lateral lung region (R-4 and L-4), the middle medial lung region (R-5 and L-5), the lower lateral lung region (R-6 and L-6), the lower medial lung region (R-7 and L-7), the upper mediastinal region (R-8 and L-8), the middle mediastinal region (R-9 and L-9), the lower mediastinal region (R-10 and L-10), and the subdiaphragmatic region (R-11 and L-11). The three main zones of the lung were (i) the peripheral zone, (ii) the central and apical zone, and (iii) the hidden zone. The peripheral zone showed the least anatomic noise and corresponded to the entire range of the R-2, R-4, R-6, L-2, L-4, and L-6 areas. The central and apical zone were partly hindered by clavicles or hilar vessels and corresponded to the entire range of the R-1, R-3, R-5, R-7, L-1, L-3, L-5, and L-7 areas. The hidden zone was entirely hindered by the heart, mediastinum, or diaphragm and corresponded to the entire range of the R-8, R-9, R-10, R-11, L-8, L-9, L-10, and L-11 areas.

and lateral regions were defined as the midline between the outer margin of the mediastinum and the lung.

Tumor diameter in the lung window (D_{lung}) was defined as the maximum diameter of the tumor in the axial plane, measured in the lung window setting (window level = −600 HU, window width = 1600 HU) (Fig. 2A). Tumor diameter in the mediastinum window (D_{med}) was defined as the maximum diameter in the mediastinum window setting (window level = 50 HU, window width = 350 HU) (Fig. 2B). Tumor size was divided into four classes: $D_{lung} \leq 2$ cm, $D_{lung} > 2$ cm and ≤ 3 cm, $D_{lung} > 3$ cm and ≤ 5 cm, and $D_{lung} > 5$ cm.

The extent of GGO was quantified by the GGO ratio: the proportion of ($D_{lung} - D_{med}$) to D_{lung}. Tumors were divided into four types on the basis of the GGO ratio: GGO-rich (GGO ratio, ≥70%), intermediate (GGO ratio, ≥30% and <70%), GGO-poor (GGO ratio, ≥10% and <30%), and solid (GGO ratio, <10%).

The tumor location was defined as one of 11 regions that included a region of interest (ROI) where the tumor existed on chest radiography (Fig. 1). When the ROI of the tumor extended over multiple regions, its location was defined as the region with the largest tumor occupation. When the tumor was not visible on a chest radiograph, the ROI of the tumor was estimated by using coronal-plane maximum-intensity projection images reconstructed from CT images.

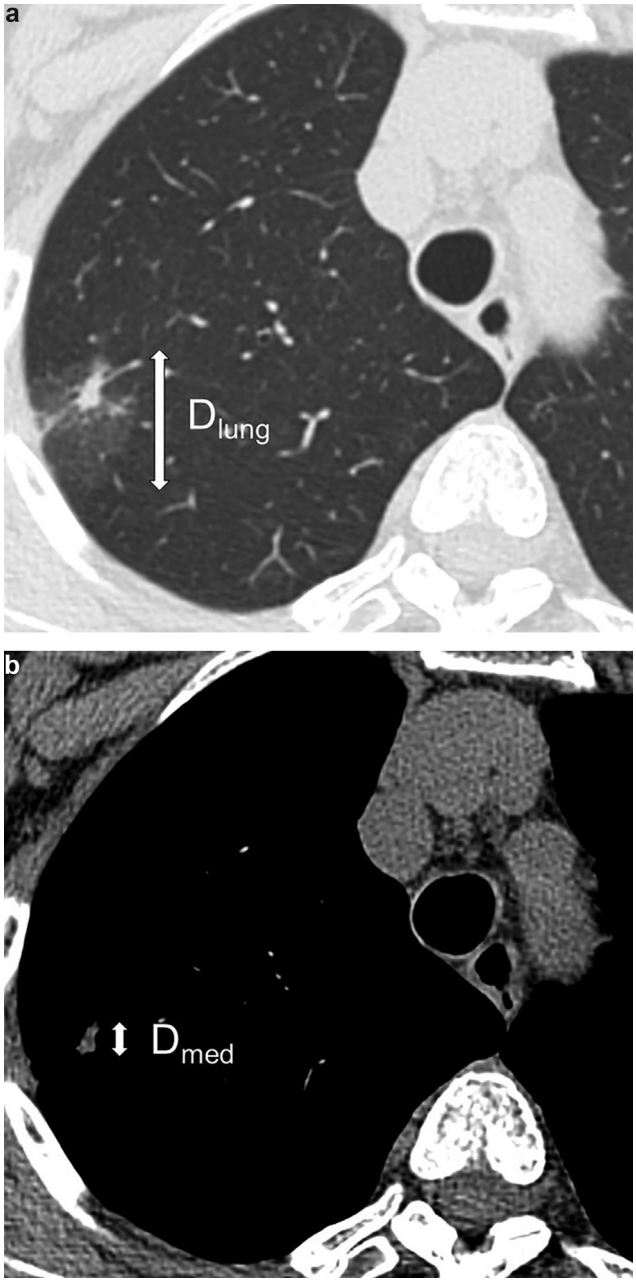

Figure 2. The tumor diameter was evaluated on 1 mm thick axial CT images without contrast enhancement in the lung and mediastinal window settings, respectively. **a**, Tumor diameter in the lung window (D_{lung}) was defined as the maximum diameter of the tumor in the axial plane measured in the lung window setting (window level = −600, window width = 1600). **b**, Tumor diameter in the mediastinum window (D_{med}) was defined as the maximum diameter in the mediastinum window setting (window level = 50, window width = 350). The extent of GGO was quantified by the GGO ratio: the proportion of ($D_{lung} - D_{med}$) to D_{lung}.

Thirteen PGY-1 trainees and nine pulmonary specialists (three radiologists, three thoracic surgeons, and three

pulmonologists) participated in this examination. All PGY-1 trainees were involved in the first year of the two-year mandatory internships at Ibaraki Prefectural Central Hospital in Japan, offering a schedule that rotates through all major and minor specialties before majoring in specialties. All pulmonary specialists were engaged in interpretation or screening examination of chest radiographs in daily clinical practice. The clinical experience of the PGY-1 trainees ranged from 2 to 12 months (mean, 8 months). The clinical experience of the specialists ranged from 9 to 41 years (mean, 23 years).

The answer sheet contained a chest radiograph scheme with 11 regions (Fig. 1). The number of tumors in each patient was not provided to examinees. Examinees were asked to mark as many regions as they suspected to contain tumors. Marks that were within the ROI of the tumor were counted as true-positive marks, whereas marks that were made outside the ROI were counted as false-positive marks. There were no true-negative marks, because each case had only one tumor. The examinees were required to take a 30 minutes ''break'' after each 50 minutes interpretation session. Images were displayed by using the radiant DICOM viewer on a monitor with an aspect ratio of 3:4 and resolution of 1536 × 2048 pixels. Zooming and panning were permitted. The evaluation of the answer sheet was performed by H. T., a board-certified radiologist who was not included among the examinees.

Standard of reference

CT findings were used for the reference standards. Tumor size and extent of GGOs were evaluated solely using the results of CT examinations. Tumor location was determined on the basis of an ROI where the tumor existed on chest radiographs and was confirmed by CT with coronal-plane maximum-intensity projection images. The number of tumors and associated lung findings in each patient were also evaluated by CT. The evaluation of reference standards was determined by mutual agreement between two radiologists (H. T. and M. M., both board-certified radiologists), who were not included among the examinees.

Statistical analysis

Student *t* test was used to compare intergroup differences in tumor detection rates. The Wilcoxon-Mann-Whitney test was used to compare intergroup differences in the sum of the detected tumors and the sum of the false-positive marks. Associations between continuous variables were investigated by using Pearson's correlation coefficient. The inter-observer agreement for the tumor detection in both groups was assessed by using the Fleiss' kappa statistics. All data were analyzed with the statistical software R (R × 64, version 3.3.2). $P < 0.05$ was considered to indicate a significant difference.

Table 1 Detected and missed tumors, false-positive counts, detection rates or sensitivities, and positive predictive values for trainees and specialists.

	Specialty	Experience	Detected tumors	Missed tumors	False-positives	Detection rate, (%)	PPV, (%)
Trainee							
1	PGY-1	2 months	103	180	216	36.4	32.3
2	PGY-1	2 months	134	149	136	47.3	49.6
3	PGY-1	2 months	136	147	289	48.1	32.0
4	PGY-1	2 months	136	147	128	48.1	51.5
5	PGY-1	2 months	131	152	201	46.3	39.5
6	PGY-1	1 year	131	152	52	46.3	71.6
7	PGY-1	1 year	127	156	75	44.9	62.9
8	PGY-1	1 year	133	150	104	47.0	56.1
9	PGY-1	1 year	127	156	96	44.9	57.0
10	PGY-1	1 year	129	154	60	45.6	68.3
11	PGY-1	1 year	133	150	57	47.0	70.0
12	PGY-1	1 year	126	157	120	44.5	51.2
13	PGY-1	1 year	117	166	246	41.3	32.2
Specialist							
1	Radiologist	9 years	162	121	15	57.2	91.5
2	Radiologist	15 years	150	133	11	53.0	93.2
3	Radiologist	30 years	161	122	55	56.9	74.5
4	Thoracic surgeon	20 years	171	112	68	60.4	71.5
5	Thoracic surgeon	23 years	182	101	56	64.3	76.5
6	Thoracic surgeon	41 years	167	116	65	59.0	72.0
7	Pulmonologist	16 years	137	146	13	48.4	91.3
8	Pulmonologist	25 years	169	114	35	59.7	82.8
9	Pulmonologist	29 years	155	128	53	54.8	74.5

Note. PPV: indicates positive predictive value; PGY: indicated post-graduate year.

Results

A total of 283 tumors was evaluated in this study, because each of the 283 patients had a solitary lung tumor. The detected and missed tumors, false-positive counts, detection rates or sensitivities and positive predictive values are summarized in Table 1.

The total numbers of detected tumors ranged from 103 (36.4%) to 136 (48.1%), with a mean of 127.9 ± 9.1 tumors (45.2 ± 3.2%) in the trainee group, and 137 (48.4%) to 182 (64.3%), with a mean of 161.6 ± 13.1 tumors (57.1 ± 4.6%) in the specialist group; the intergroup difference was statistically significant ($P < 0.001$). The Fleiss' kappa statistics of tumor detection were 0.72 in the trainee group and 0.75 in the specialist group. In the specialist group, the number of tumors detected by radiologists was 157.7 (range: 150—162 tumors); by thoracic surgeons, 173.3 (range: 167—182 tumors); and by pulmonologists, 153.7 (range: 137—169 tumors). The number of detected tumors demonstrated a weak correlation with clinical experience in the specialist group ($r = 0.30$), but no correlation with clinical experience in the trainee group ($r = -0.01$). The total numbers of false-positive marks for all cases were 52—289 (mean: 137.8, median: 120) in the trainee group and 11—68 (mean: 41.2, median: 53) in the specialist group ($P < 0.001$). The numbers of false-positive marks in the peripheral zone were 4—129 (mean: 20.2, median: 8) in the trainee group and 1—29 (mean: 10.7, median: 10) in the specialist group ($P = 0.781$). The numbers of false-positive marks in the central and apical zone were 37—229 (mean: 99.0, median: 91) in the trainee group and 8—50 (mean: 25.1, median: 31) in the specialist group ($P < 0.001$). The numbers of false-positive marks in the hidden zone were 4—60 (mean: 18.6, median: 15) in the trainee group and 1—9 (mean: 5.3, median: 5) in the specialist group ($P = 0.006$). In the specialist group, the number of false-positive marks by radiologists was 11—55 (mean: 27.0); by thoracic surgeons, 56—68 (mean: 63); and by pulmonologists, 13—53 (mean: 33.7). The number of false-positive marks demonstrated strong positive correlation with clinical experience in the specialist group ($r = 0.74$), and strong negative correlation with clinical experience in the trainee group ($r = -0.62$).

The intergroup detectability differences for each tumor category are summarized in Table 2 and displayed in Fig. 3, and pathological diagnosis of the tumor in each tumor category is summarized in Table 3. Tumor categories that showed statistically significant intergroup detectability differences were:

- intermediate and GGO-poor tumors of any size in the peripheral zone (Fig. 4);
- solid tumors with $D_{lung} \leq 2$ cm in the peripheral zone (Fig. 5);
- intermediate tumors with $D_{lung} > 3$ cm and ≤ 5 cm in the central and apical zone;
- GGO-poor tumors with $D_{lung} \leq 2$ cm in the central and apical zone (Fig. 6);
- solid tumors with $D_{lung} > 2$ cm and ≤ 5 cm in the central and apical zone;
- GGO-poor tumors with $D_{lung} > 3$ cm in the hidden zone, and;
- solid tumors with $D_{lung} > 2$ cm and ≤ 5 cm in the hidden zone.

Discussion

Our study investigated imaging characteristics of lung tumors that influenced experience-related differences in detectability. Tumors were classified into each category on the basis of size on CT scans, GGO ratio on CT, and location on chest radiograph. The detection rates between PGY-1 trainees and pulmonary specialists, including radiologists, thoracic surgeons, and pulmonologists, were compared in each tumor category. The basic concept of our study was to analyze the influence of radiologic expertise in detecting malignant lung tumors, which would contribute to improvement of the training course for chest radiographs in post-graduate medical education.

In our study, intermediate and GGO-poor tumors in the peripheral zone, of any size yielded statistically significant intergroup detectability differences of >10%. The conspicuousness or extent of GGO has previously been reported to affect the detectability of lung tumors on chest radiographs [6—8,13,14]. Austin et al. reported that the majority of missed lesions on chest radiographs were not completely well-defined [13]. Our study added new findings: experience-related differences in detectability also increase in conspicuous tumors, with GGO ratios ranging from 10% to 70%. Further, solid tumors with $D_{lung} \leq 2$ cm also showed statistically significant intergroup detectability differences of 14.3%. Previous studies have reported poor detectability of small lung nodules on chest radiographs. Hayashi et al. demonstrated that the median size of undetectable lung cancer on chest radiographs was 14 mm [14]. Other reports have described varying average diameter values for missed carcinomas, such as 21 ± 0.9 mm [16], and 16 ± 8 mm [13]. Our study reveals that experience-related differences in detectability also increase for small peripheral well-defined tumors with diameter ≤2 cm. On the opposite, solid tumors with $D_{lung} > 2$ cm in the peripheral zone have mean detectability > 98% in both groups and a non-significant intergroup detectability difference of < 1.9%. This result suggests that well-defined peripheral tumors with diameter > 2 cm are easily detectable on chest radiography without specific training.

In the central and apical zone, the number of tumor categories that showed statistically significant intergroup detectability differences was lower than in the peripheral zone. This is partly because trainees tend to emphasize abnormalities in this zone, because they are not aware that false-positives might occasionally occur here due to the existence of pulmonary vasculature and costal cartilage ossification. This hypothesis was supported by false-positive counts in the trainee group that were significantly larger in the central and apical zone (range: 37—229, mean: 99.0, median: 91) than in the peripheral (range: 4—129, mean: 20.2, median: 8) and hidden zones (range: 4—60, mean: 18.6, median: 15), and the overall difference of false-positive counts between the trainee and specialist groups was statistically significant in the central and apical zone ($P < 0.001$). Furthermore, among cases located in the central and apical zone, the proportions of areas of lung tumors hidden by anatomic noise on chest radiographs greatly differed. Thus, for the detection of tumors in the central and apical zone, trainees must learn the approach for distinguishing true-positive and false-positive findings.

Table 2 Detection rates for trainees and specialists, with corresponding statistical significance. Tumor categories were classified on the basis of ground glass opacity (GGO) ratio (GGO-rich, intermediate, GGO-poor, and solid types), tumor size (using Dlung values), and tumor location on chest radiographs.

		Peripheral					
		n	Trainees		Specialists		
	Tumor size (D_{lung})	129	Detected case	Detection rate %	Detected case	Detection rate %	*P*-value
GGO-rich (*n* = 46)	≤2 cm	17	0.2 (0—1)	0.9 (0—5.9)	0.8 (0—2)	4.6 (0—11.8)	0.061
	≤3 cm >2 cm	4	0.1 (0—1)	1.9 (0—25)	0.3 (0—1)	8.3 (0—25)	0.138
	≤5 cm >3 cm	0	N/A	N/A	N/A	N/A	N/A
Intermediate(*n* = 55)	≤ cm	19	4.5 (2—7)	23.9 (10.5—36.8)	9.8 (8—12)	51.5 (42.1—63.2)	<0.001[a]
	≤3 cm >2 cm	7	1.2 (0—2)	17.6 (0—28.6)	5.0 (3—6)	71.4 (42.9—85.7)	<0.001[a]
	≤5 cm >3 cm	3	1.2 (0—2)	38.5 (0—66.7)	2.3 (1—3)	77.8 (33.3—100)	0.002[a]
	>5 cm	0	N/A	N/A	N/A	N/A	N/A
GGO-poor (*n* = 93)	≤2 cm	18	8.6 (5—11)	47.9 (27.8—61.1)	11.2 (8—15)	62.3 (44.4—83.3)	0.005[a]
	≤3 cm >2 cm	15	10.2 (7—13)	67.7 (46.7—86.7)	12.4 (11—14)	83.0 (73.3—93.3)	0.001[a]
	≤5 cm >3 cm	13	10.8 (8—12)	83.4 (61.5—92.3)	12.6 (12,13)	96.6 (92.3—100)	<0.001[a]
	>5 cm	2	1.4 (1,2)	69.2 (50.0—100)	1.9 (1,2)	94.4 (50.0—100)	0.017[a]
Solid (*n* = 89)	≤2 cm	8	5.4 (3—6)	67.3 (37.5—75.0)	6.6 (5—8)	81.9 (62.5—100)	0.009[a]
	≤3 cm >2 cm	10	9.9 (9,10)	99.2 (90.0—100)	9.9 (9,10)	98.9 (90.0—100)	0.796
	≤5 cm >3 cm	8	7.8 (7,8)	98.1 (87.5—100)	8 (8)	100 (100)	0.237
	>5 cm	5	5 (5)	100 (100)	5 (5)	100 (100)	N/A

Table 2 (*Continued*)

		Central and apical					
		n	Trainees		Specialists		
	Tumor size (D_{lung})	127	Detected case	Detection rate %	Detected case	Detection rate %	*P*-value
GGO-rich (*n* = 46)	≤2 cm	16	0.1 (0—1)	0.5 (0—6.3)	0.1 (0—1)	0.7 (0—6.3)	0.796
	≤3 cm >2 cm	6	0.2 (0—1)	2.6 (0—16.7)	0.4 (0—1)	7.4 (0—16.7)	0.146
	≤5 cm >3 cm	1	0 (0)	0 (0)	0 (0)	0 (0)	N/A
Intermediate(*n* = 55)	≤2 cm	6	0.4 (0—1)	6.4 (0—16.7)	0.2 (0—1)	3.7 (0—16.7)	0.446
	≤3 cm >2 cm	10	1.4 (0—3)	13.8 (0—30.0)	1.8 (0—4)	17.8 (0—40.0)	0.404
	≤5 cm >3 cm	5	2.1 (0—3)	41.5 (20.0—60.0)	3.2 (1—4)	64.4 (20.0—80.0)	0.006[a]
	>5 cm	1	0.8 (0—1)	84.6 (0—100)	0.9 (0—1)	88.9 (0—100)	0.787
GGO-poor (*n* = 93)	≤2 cm	13	3.3 (2—4)	25.4 (15.4—30.8)	5.9 (4—8)	45.3 (30.8—61.5)	<0.001[a]
	≤3 cm >2 cm	8	4.1 (2—7)	51.0 (25.0—87.5)	4.0 (3—6)	50.0 (37.5—75)	0.875
	≤5 cm >3 cm	12	8.4 (7—10)	69.9 (58.3—83.3)	9.2 (7—11)	76.9 (58.3—91.7)	0.110
	>5 cm	2	1.9 (1,2)	96.2 (50.0—100)	2 (2)	100 (100)	0.419
Solid (*n* = 89)	≤2 cm	4	1.8 (0—4)	46.2 (0—100)	2.6 (1—4)	63.9 (25.0—100)	0.134
	≤3 cm >2 cm	12	7 (4—9)	58.3 (33.3—75.0)	9.2 (7—11)	76.9 (58.3—91.7)	0.001[a]
	≤5 cm >3 cm	21	16.6 (13—19)	79.1 (61.9—90.5)	19.7 (19,20)	93.7 (90.5—95.2)	<0.001[a]
	>5 cm	10	9.9 (9,10)	99.2 (90.0—100)	10 (10)	100 (100)	0.419

Table 2 (*Continued*)

		Hidden					
		n	Trainees		Specialists		
	Tumor size (D_{lung})	27	Detected case	Detection rate %	Detected case	Detection rate %	*P*-value
GGO-rich (*n* = 46)	≤2 cm	2	0 (0)	0 (0)	0 (0)	0 (0)	N/A
	≤3 cm >2 cm	0	N/A	N/A	N/A	N/A	N/A
	≤5 cm >3 cm	0	N/A	N/A	N/A	N/A	N/A
Intermediate(*n* = 55)	≤2 cm	1	0 (0)	0 (0)	0 (0)	0 (0)	N/A
	≤3 cm >2 cm	3	0.1 (0—1)	2.6 (0—33.3)	0 (0)	0 (0)	0.419
	≤5 cm >3 cm	0	N/A	N/A	N/A	N/A	N/A
	>5 cm	0	N/A	N/A	N/A	N/A	N/A
GGO-poor (*n* = 93)	≤2 cm	3	0 (0)	0 (0)	0.2 (0—1)	7.4 (0—33.3)	0.081
	≤3 cm >2 cm	4	0.9 (0—2)	23.1 (0—50.0)	1.2 (1,2)	30.6 (25—50)	0.16
	≤5 cm >3 cm	2	0 (0)	0 (0)	0.4 (0—2)	22.2 (0—100)	0.037[a]
	>5 cm	1	0 (0)	0 (0)	0.3 (0—1)	33.3 (0—100)	0.025[a]
Solid (*n* = 89)	≤2 cm	3	0.3 (0—1)	10.3 (0—33.3)	0.1 (0—1)	3.7 (0—33.3)	0.302
	≤3 cm >2 cm	5	0.5 (0—2)	9.2 (0—40.0)	1.2 (0—2)	24.4 (0—40.0)	0.015[a]
	≤5 cm >3 cm	3	1.8 (0—3)	61.5 (0—100)	3 (3)	100 (100)	0.002[a]
	>5 cm	0	N/A	N/A	N/A	N/A	N/A

Note: Numbers in brackets are the ranges. The second decimal places were rounded off in detected case and detection rate. GGO: indicates ground glass opacity.

[a] Statistically significant ($P < 0.05$).

Table 3 Pathological diagnoses for the four tumor types: ground glass opacity (GGO)-rich, intermediate, GGO-poor, and solid.

	GGO-rich ($n = 46$)	Intermediate ($n = 55$)	GGO-poor ($n = 93$)	Solid ($n = 89$)
Adenocarcinoma, (n = 207)	**46**	**53**	**66**	**42**
Nonmucinous AIS, ($n = 31$)	*21*	*10*	*0*	*0*
Mucinous AIS, ($n = 2$)	*0*	*2*	*0*	*0*
Nonmucinous MIA, ($n = 45$)	*23*	*16*	*6*	*0*
Mucinous MIA, ($n = 3$)	*0*	*1*	*1*	*1*
Lipidic invasive adenocarcinoma, ($n = 36$)	*1*	*15*	*16*	*4*
Papillary invasive adenocarcinoma, ($n = 13$)	*1*	*1*	*6*	*5*
Acinar invasive adenocarcinoma, ($n = 32$)	*0*	*4*	*17*	*11*
Micropapillary invasive adenocarcinoma, ($n = 8$)	*0*	*1*	*3*	*4*
Solid invasive adenocarcinoma, ($n = 26$)	*0*	*1*	*11*	*14*
Mucinous invasive adenocarcinoma, ($n = 11$)	*0*	*2*	*6*	*3*
Non-adenocarcinoma, (n = 76)	**0**	**2**	**27**	**47**
Squamous cell carcinoma, ($n = 57$)	*0*	*1*	*21*	*35*
Small cell carcinoma with combined small cell carcinoma, ($n = 8$)	*0*	*0*	*3*	*5*
LCNEC with combined LCNEC, ($n = 3$)	*0*	*0*	*0*	*3*
Others, ($n = 8$)	*0*	*1*	*3*	*4*

Note. AIS: indicates adenocarcinoma in situ; MIA: indicates minimally invasive adenocarcinoma; LCNEC: indicates large cell neuroendocrine carcinoma; GGO: indicates ground glass opacity. Bold indicates total numbers.

The search for tumors obscured by heart, mediastinum, or diaphragm, known as the ''hide-and-seek'' tumors, has been a core educational topic in the interpretation of chest radiographs [18—20]. Our study reveals that tumors in the hidden zone with statistically significant intergroup detectability differences of >10% are limited to GGO-poor type tumors with $D_{lung} > 3$ cm and solid tumors with $D_{lung} > 2$ cm. In contrast, intermediate

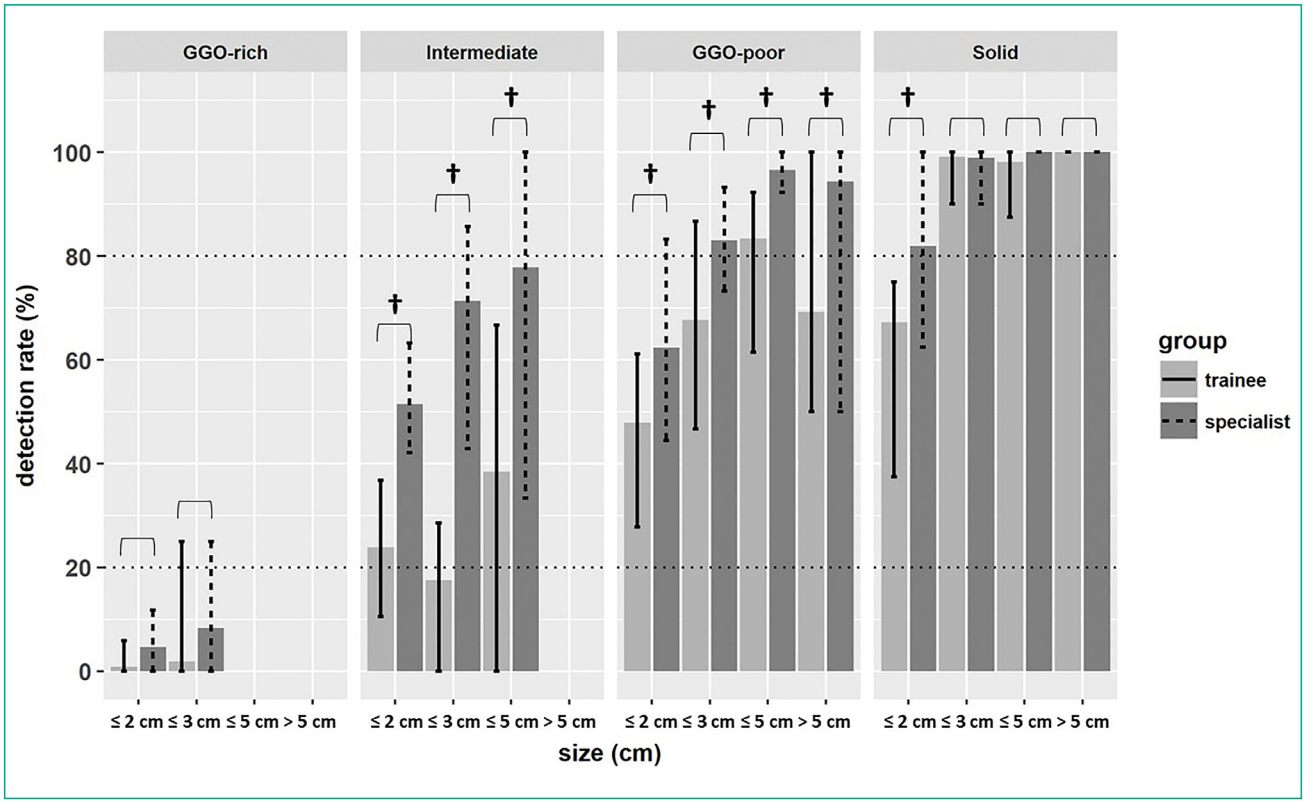

Figure 3. Graphs show detection rates of lung tumors on chest radiographs in the different zones. **a**. Peripheral zone. **b**. Central and apical zone. **c**. Hidden zone.

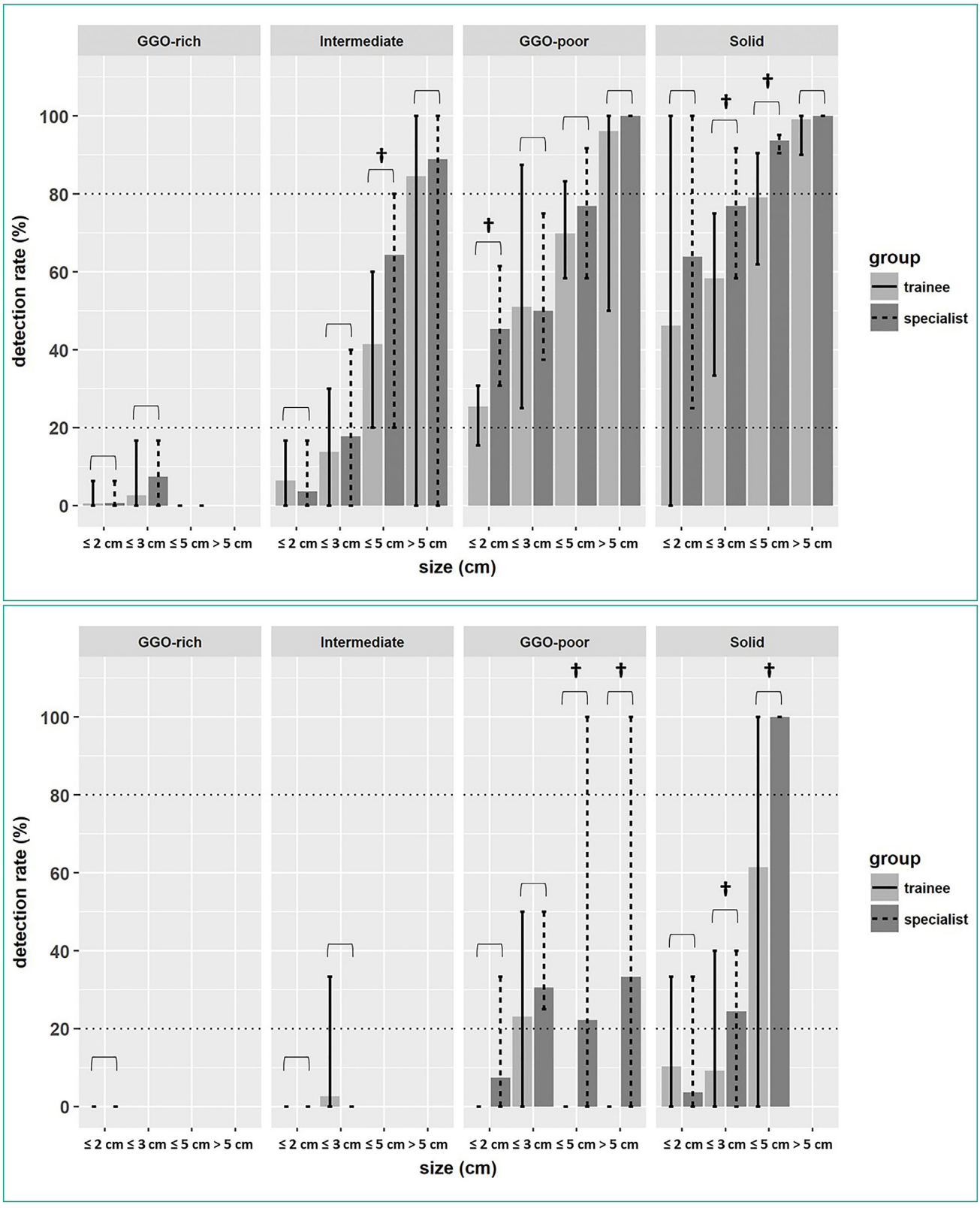

Figure 3. (*Continued*)

tumors of any size and tumors of any type with D_{lung} ≤2 cm showed average detectability ranging between 0% and 10.3% in both groups, without significant inter-group difference in detectability. This result suggests that hidden tumors with conspicuous margins or small sizes are not detectable on chest radiographs, even for those with adequate experience in chest radiography interpretation.

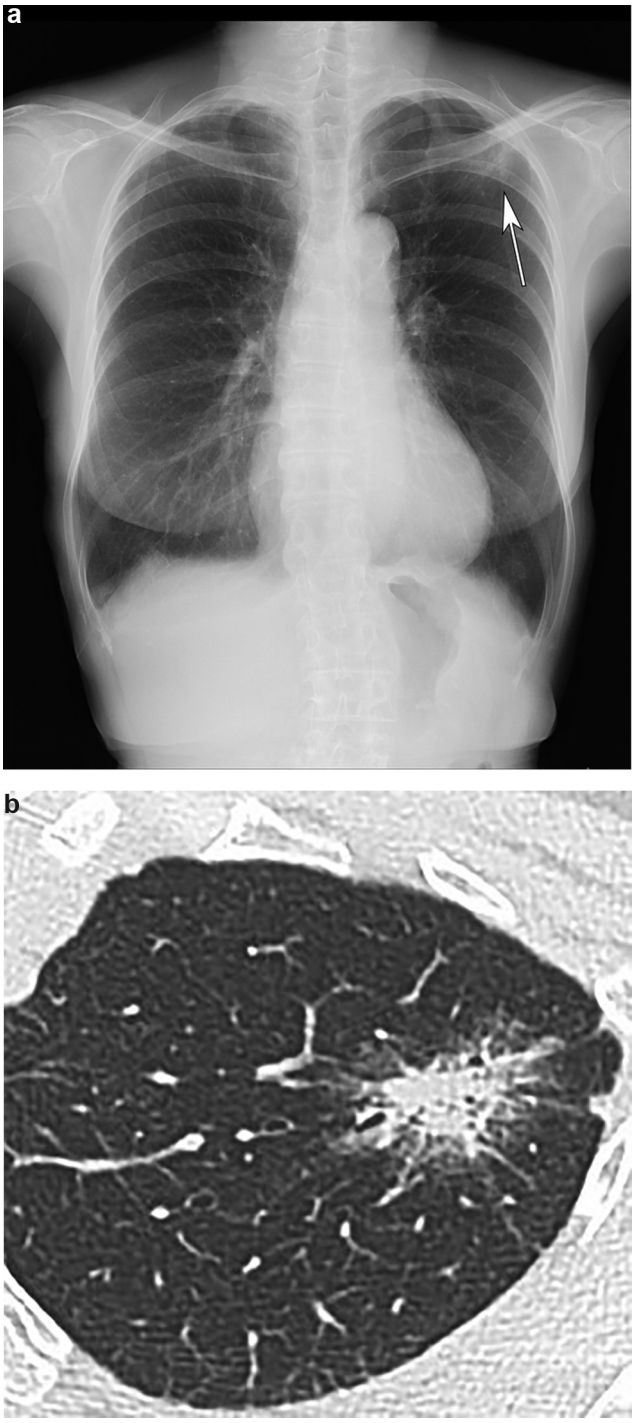

Figure 4. A. Chest X ray shows lung tumor located in the peripheral zone (L-2) on chest radiography. B. Its D_{lung} was 40 mm, D_{med} was 25 mm, and ground glass opacity (GGO) ratio was 37.5% (intermediate type). The tumor was pathologically diagnosed as an invasive lepidic adenocarcinoma. Eight of 13 trainees and all nine specialists identified the tumor.

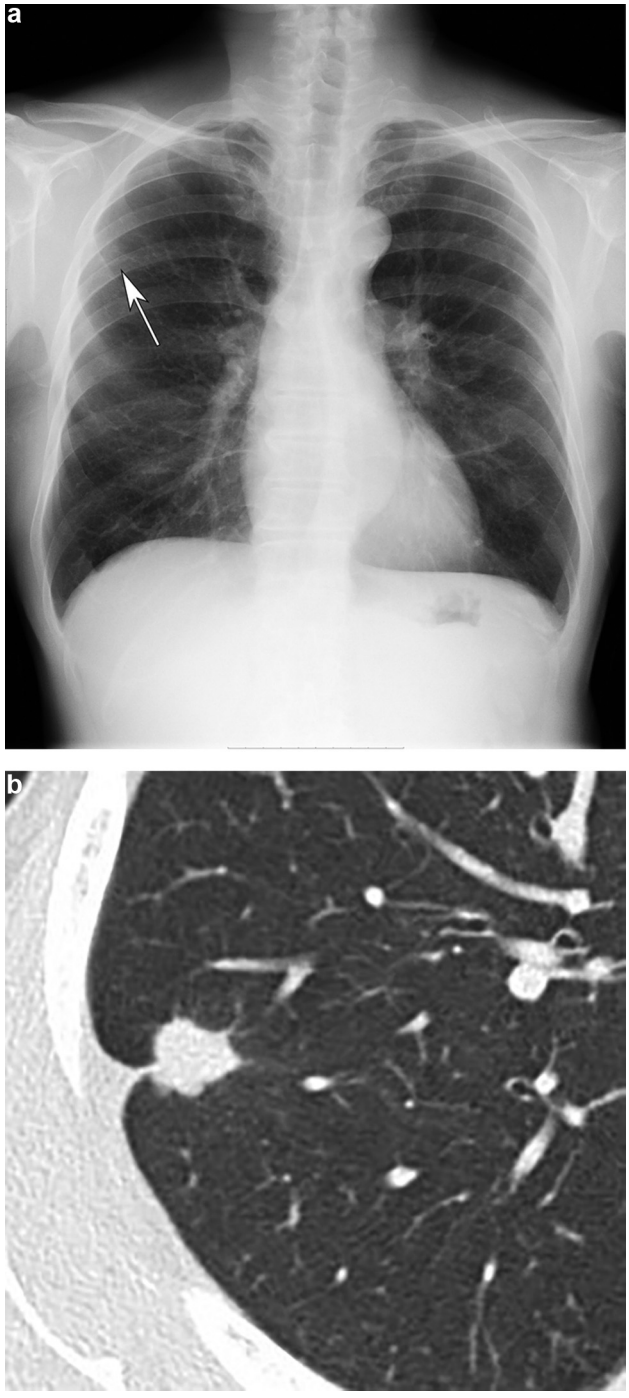

Figure 5. a,. Chest X ray shows lung tumor located in the peripheral zone (R-2) (arrow). **b**, Its D_{lung} was 15 mm, D_{med} was 14 mm, and ground glass opacity (GGO) ratio was 6.7% (solid type). The tumor was pathologically diagnosed as an invasive lepidic adenocarcinoma. None of the 13 trainees and 4 of 9 specialists identified the tumor.

Regardless of location and size, GGO-rich tumors yielded average detectability of <10% in both groups, without significant intergroup difference in detectability. In a previous study, tumors with GGO ratios of ≥70% on thin-section CT were difficult to detect on chest radiography [7,14]. Our study reveals that experience-related differences in detectability are slight in tumors with GGO ratio of ≥70%. In addition, all GGO-rich tumors were histologically diagnosed as adenocarcinomas; only two of 46 cases (4.3%) were invasive adenocarcinomas. Therefore, even if the GGO-rich tumors are not depicted on chest radiographs in daily clinical practice, most are considered non-life-threatening adenocarcinomas [21].

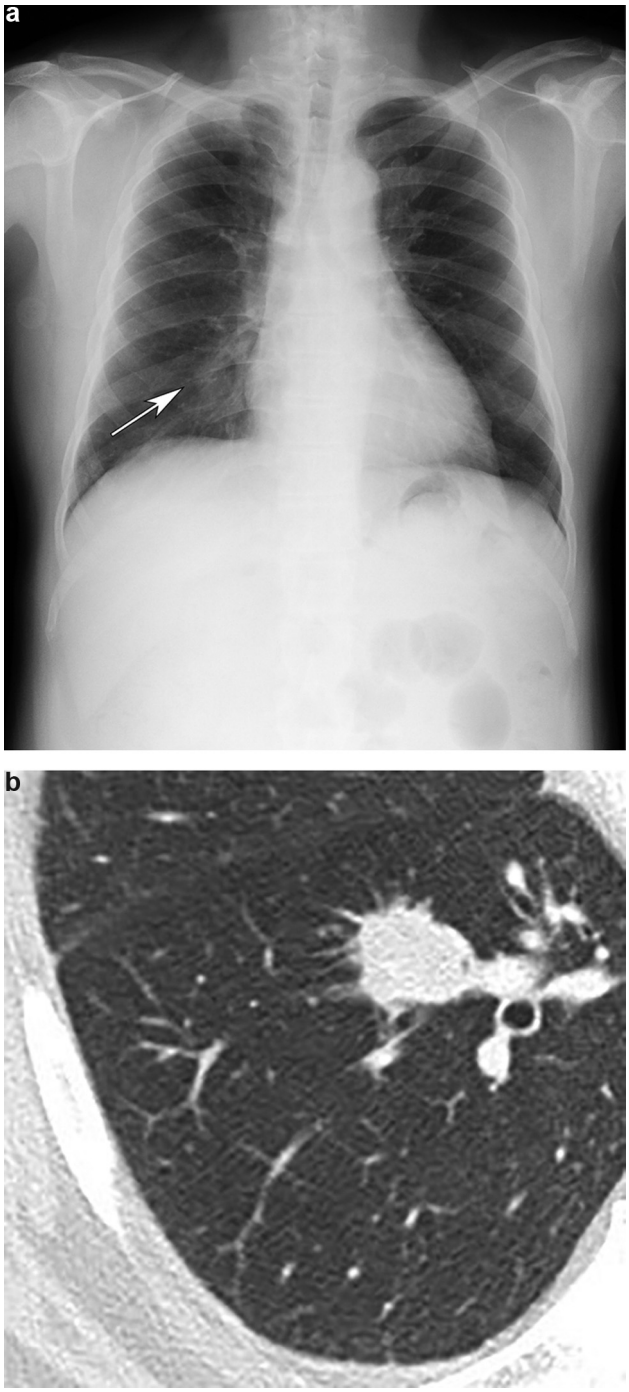

Figure 6. Chest X ray shows lung tumor located in the central and apical zone (R-7) (arrow). **b**, Its D_{lung} was 19 mm, D_{med} was 17 mm, and ground glass opacity (GGO) ratio was 10.5% (GGO-poor type). The tumor was pathologically diagnosed as a squamous cell carcinoma. Five of 13 trainees and seven of nine specialists identified the tumor. The tumor was partly hindered by pulmonary vasculature.

Our study had some limitations. First, we included different types and experience levels of experts in the specialist group. The number of years of experience had positive influence on the detection of tumors and negative influence on false-positive marks. Thoracic surgeons had greater numbers of detected tumors and false-positive marks, compared with radiologists and pulmonologists. Thus, it seems that there is a difference in recognition method among expert types and years of experience. Second, readers were informed that the lesions they were investigating were limited to lung tumors. In the clinical setting, interpreters typically do not know the findings on the chest radiograph in advance. Third, false-positive marks may have been mistakenly counted as true-positive in some cases by the evaluator, if the readers coincidentally marked the false-positive findings which were located exactly in the same area where the ROI of the tumor existed.

In conclusion, our study assessed differences in lung tumor detectability on chest radiographs between trainees and specialists on the basis of tumor size, extent of GGO, and tumor location. A thorough understanding of these results may lead to improvements in training protocols for chest radiography in post-graduate medical education.

Acknowledgements

Motohiro Sato, M.D. kindly provided important advice for the study design.

Ryuta Amemiya, M.D. (Ibaraki Prefectural Central Hospital, Department of Thoracic Surgery), Hisashi Suzuki, M.D. (Ibaraki Prefectural Central Hospital, Department of Thoracic Surgery), Ikuta Hashimoto, M.D (Ibaraki Prefectural Central Hospital, Department of Respiratory Medicine), Shozaburo Yamaguchi M.D. (Ibaraki Prefectural Central Hospital, Department of Respiratory Medicine), Satoshi Morinaka M.D., Daisuke Yamamoto M.D., Gentaro Nagano M.D., Honoka Kotoku M.D., Moe Ogimoto M.D., Shoko Takahashi M.D., Naoki Ishibashi M.D., Chio Sakai M.D., Hironobu Yamazaki M.D., Shota Noguchi M.D., Shota Yamashita M.D., Yusuke Iguchi M.D., and Keisuke Shimizu M.D. kindly participated as the examinees in this study.

Disclosure of interest

The authors declare that they have no competing interest.

References

[1] Gohagan JK, Marcus PM, Fagerstrom RM, et al. Final results of the Lung Screening Study, a randomized feasibility study of spiral CT versus chest X-ray screening for lung cancer. Lung Cancer 2005;47:9—15.
[2] Croswell JM, Baker SG, Marcus PM, Clapp JD, Kramer BS. Cumulative incidence of false-positive test results in lung cancer screening: a randomized trial. Ann Intern Med 2010;152:505—12.
[3] Sone S, Takashima S, Li F, et al. Mass screening for lung cancer with mobile spiral computed tomography scanner. Lancet 1998;351:1242—5.
[4] Henschke CI, McCauley DI, Yankelevitz DF, et al. Early lung cancer action project: overall design and findings from baseline screening. Lancet 1999;354:99—105.
[5] Chassagnon G, Revel MP. Time to get back to basics and teach chest X-ray! Diagn Interv Imaging 2018;99:347—8.
[6] Wu MH, Gotway MB, Lee TJ, et al. Features of non-small cell lung carcinomas overlooked at digital chest radiography. Clin Radiol 2008;63:518—28.

[7] Tsubamoto M, Kuriyama K, Kido S, et al. Detection of lung cancer on chest radiographs: analysis on the basis of size and extent of ground-glass opacity at thin-section CT. Radiology 2002;224:139—44.
[8] Del Ciello A, Franchi P, Contegiacomo A, Cicchetti G, Bonomo L, Larici AR. Missed lung cancer: when, where, and why? Diagn Interv Radiol 2017;23:118—26.
[9] Monnier-Cholley L, Carrat F, Cholley BP, Tubiana JM, Arrive L. Detection of lung cancer on radiographs: receiver operating characteristic analyses of radiologists', pulmonologists', and anesthesiologists' performance. Radiology 2004;233:799—805.
[10] Kundel HL, Nodine CF. Interpreting chest radiographs without visual search. Radiology 1975;116:527—32.
[11] Kelly BS, Rainford LA, Darcy SP, Kavanagh EC, Toomey RJ. The development of expertise in radiology: in chest radiograph interpretation ''expert'' search pattern may predate ''expert'' levels of diagnostic accuracy for pneumothorax identification. Radiology 2016;280:252—60.
[12] Fabre C, Proisy M, Chapuis C, Jouneau S, Lentz PA, Meunier C, et al. Radiology residents' skill level in chest x-ray reading. Diagn Interv Imaging 2018;99:361—70.
[13] Austin JH, Romney BM, Goldsmith LS. Missed bronchogenic carcinoma: radiographic findings in 27 patients with a potentially resectable lesion evident in retrospect. Radiology 1992;182:115—22.
[14] Hayashi H, Ashizawa K, Uetani M, et al. Detectability of peripheral lung cancer on chest radiographs: effect of the size, location and extent of ground-glass opacity. Br J Radiol 2009;82:272—8.
[15] Muhm JR, Miller WE, Fontana RS, Sanderson DR, Uhlenhopp MA. Lung cancer detected during a screening program using four-month chest radiographs. Radiology 1983;148:609—15.
[16] Shah PK, Austin JH, White CS, et al. Missed non-small cell lung cancer: radiographic findings of potentially resectable lesions evident only in retrospect. Radiology 2003;226:235—41.
[17] Travis WD, Brambilla E, Nicholson AG, et al. The 2015 World Health Organization Classification of Lung Tumors: impact of genetic, clinical and radiologic advances since the 2004 classification. J Thorac Oncol 2015;10:1243—60.
[18] Oetreich AE. A helpful hint for chest radiology: ''look behind the heart''. J Natl Med Assoc 1982;74:1029—31.
[19] Gibbs JM, Chandrasekhar CA, Ferguson EC, et al. Lines and stripes: where did they go? From conventional radiography to CT. Radiographics 2007;27:33—48.
[20] Chotas HG, Ravin CE. Chest radiography: estimated lung volume and projected area obscured by the heart, mediastinum, and diaphragm. Radiology 1994;193:403—4.
[21] Kadota K, Villena-Vargas J, Yoshizawa A, et al. Prognostic significance of adenocarcinoma in situ, minimally invasive adenocarcinoma, and nonmucinous lepidic predominant invasive adenocarcinoma of the lung in patients with stage I disease. Am J Surg Pathol 2014;38:448—60.